# 5. CHARACTERIZATION OF FRACTURE TOUGHNESS BY DEVELOPED DEFORMATION AT CRACK EXTENSION; COMPARISON WITH ENERGY BALANCE CONSIDERATIONS.

H.C. van Elst, Metal Research Institute TNO, P.B. 541, Apeldoorn, Netherlands

ABSTRACT

The fracture resistance of a material is quantitatively related to the elongation caused by the wake of an extended crack; this is considered an alternative for the well-known COD approach. This analysis in principle also implies the calculation of fracture toughness from the stress-strain response of the material (at relevant strain rate). Restrictions conditioning 'valid' determinations appear comparable, but more transparent than with $J_{Ic}$-determinations. A comparison with energy balance considerations offers consistent results. The application of these fracture resistance estimates for the case of ductile behaviour involving a fully yielded ligament is discussed.

Nomenclature:

| Symbol | Refers to observable |
|---|---|
| P | load |
| $\sigma$ | stress |
| f | deflection |
| A | performed work |
| a | cracklength |
| U | elastic energy |
| V | kinetic energy |
| W | dissipated energy |
| H | absorbed energy |
| C | compliance |
| w | width (of specimen) |
| b | thickness (of specimen) |
| h | height (of specimen) |
| R | crack extension resistance |
| r | crack initiation resistance |
| $\rho$ | average (global) crack extension resistance for complete separation |
| $\rho^*$ | average (global) crack resistance including initiation for complete separation |
| $\varepsilon$ | deformation |

| Index | To observable | Refers to |
|---|---|---|
| 0 | a,w,h,b | initial value |
| | $\sigma$ | 'gross' stress |
| | $\phi$ | centre pipe diameter |
| e | R,W | crack extension |
| i | W,f | crack initiation |
| U | f,C,R | elastic |
| W | f,C,R | plastic |
| V | R | kinetic |
| a | r,R,W | dissipative processes required by crack processes only (crack initiation and crack surface realization at extension) |
| | f | cracklength a |
| q | r,R,W | dissipative processes due to material reaction forces of external load, causing yield (and accompanying the crack (a)-processes) |
| w | f | cracklength a=w |
| $\sim$ | $\sigma,\varepsilon$ | circumferential |
| B | y,g | elastic plastic boundary |



Nomenclature (cont'd)

| Symbol | Refers to observable |
|---|---|
| $\varepsilon^*$ | effective deformation |
| e | energy density |
| n | strain hardening exponent |
| k | constant of Davidenkov-Ludwik |
| g | polar radius from crack tip origin |
| $\theta$ | angle between g and a |
| $\gamma$ | g/a |
| Y | uniaxial yield strength |

| Index | To observable | Refers to |
|---|---|---|
| k,j | $R,r,\rho,\rho^*$ | relevant term indication for coefficients in series expansion of $W,R,\sigma,\rho,\rho^*$ in $(a-a_o)$ and (or) $w-a_o$ |

## 1. INTRODUCTION

Our interest is the resistance against ductile fracture propagation, in particular with respect to such failure of gaspressurized pipelines under steady state conditions. This (large scale) shear fracture implies instability not due to a relaxation of elastic energy stored in the material, which would be quite insufficient in magnitude, but due to the continuous performance of work drawn on the energy of the compressed gas at crack extension. This phenomenon has been reviewed in literature by several authors. Cf. a.o. [1], [2], [3], [4], [5], [6], [7]. For an appraisal of the risk of such a failure the knowledge of the energy dissipation per unit crack extension (and per unit pipe wall thickness) will be of paramount importance. To evaluate this fracture resistance for the ductile mode, displacement controlled tests on fracture mechanics (like CT-, DCB- and CN-) specimens of linepipe steel were performed. By suitable instrumentation it proved possible to record in a synchroneous way: load, displacement and cracklength in time. An energy balance analysis as elaborated sub 3 will then allow to determine the dissipated energy as a function of crack extension. Two difficulties arise:

1. A marked influence of geometry and dimension (in particular ligament size) is present.
2. The energy dissipation proceeds by two types of macro mechanisms; viz.:
   a) by the from conventional fracture mechanics well-known development of the plastic zone at the crack tip, as required for the realization of fracture surface. (This accounts for the 'real' fracture resistance corresponding with the effective surface energy: 'a-dissipation' related to the crack a.).

b) by material reaction forces to the external load, these becoming so high in this ductile material to achieve crack extension, that they cause yield also in absence of the stress intensity action, i.e. remote from the crack. (An increase of the radius of the crack tip would hardly influence this 'q-dissipation').

Both types of energy dissipation presumably obey different geometrical laws. If ρ, the crack tip radius increases, the q-energy dissipation contribution will increase. For f.m.-specimens involving bending (like SENB-, CT-, DCB-specimen) the compressed region at the free surface opposite to the cracktip, when yielding, involves 'q-dissipation'. The plastic bending of the torn parts in DCB-specimen when inducing crack extension by increase of displacement - and also the flattening of the torn pipe part behind the moving cracktip for a failing pipe - adds in an unavoidable way to the energy dissipation during crack extension in a 'q-process' fashion. While the a-dissipation refers to an effective energy surface times crack surface, the q-dissipation refers to an (average) energy density times a volume.
It was tried to seperate the 'real' fracture mechanics fracture resistance $R_a$, directly linked to the crack, from the total ('apparent') fracture resistance: $R = R_a + R_q$. Stiffened and side grooved specimens were used to suppress q-energy dissipation. By a plastic stress-strain analysis an evaluation of the q-energy dissipation (as e.g. in the case of the tearing pipe) can be tried. Thus if $R_a$ is found from experiments the 'apparent' R can be estimated. In the performed experiments, the q-processes were always already present before initiation.

## 2. ON THE RELATION BETWEEN THE (REAL) FRACTURE PROPAGATION RESISTANCE $R_a$ AND THE STRESS-STRAIN-STRAIN RATE PERFORMANCE OF THE MATERIAL UNDER UNIAXIAL LOADING

If a crack extends the accompanying movement of the plastic zone at the cracktip leaves a wake of plastically deformed material along the sides of the crackpath. Without interfering with the principle of the following argument a crack extending with constant velocity $\dot{a}$ in the x-direction (e.g. in an unstable way) is considered and the plastic zone at the crack tip is assumed to be contained and to remain the same; unit thickness is taken and deformation gradients in the thickness direction are neglected. The above-mentioned wake of plastically deformed material will be caused by the sweeping of a 'curve' $\Gamma = \Gamma(x,y)$ within the plastic zone, being the locus of points showing maximum density of energy dissipation $e_\Gamma(x,y)$ on lines parallel to the crack for the static case and in a conventional



schematic 2-dimensional picture. Cf. fig. 2.1. Apparently Γ emerges in two directions from the cracktip and ends on those points $P_{1,2}$ of the elastic-plastic boundary $y_B = y_B(x)$ for which $\frac{dy_B}{dx} = 0$. With:

$$e_\Gamma(x,y) = \int_0^{\varepsilon^*_\Gamma(x,y)} Y d\varepsilon^*_\Gamma \quad \ldots\ldots\ldots\ldots\ldots\ldots\ldots \quad (2.1)$$

this locus will obey:

$$\left(\frac{\partial e_\Gamma}{\partial x}\right)_y = Y\left(\frac{\partial \varepsilon_n{}^*(x,y)}{\partial x}\right)_y = 0 \quad \ldots\ldots\ldots\ldots\ldots\ldots\ldots \quad (2.2)$$

Here $\varepsilon^*$ = effective deformation. Thus with $\varepsilon_1$ and $\varepsilon_2$ principal natural strains:

$$d\varepsilon^* = \frac{2}{3}\sqrt{3}\sqrt{d\varepsilon_1{}^2 + d\varepsilon_1 d\varepsilon_2 + d\varepsilon_2{}^2}$$

As here $\varepsilon_2 \simeq 0$, $d\varepsilon^* \simeq \frac{2}{3}\sqrt{3}\, d\varepsilon_1$ ( Y= uniaxial yield strength).

Apparently the energy dissipation pro unit of crack path has been:

$$R = \int_\Gamma dy \int_0^{\varepsilon^*_\Gamma(x,\bar{y})} Y d\varepsilon^* = \int_\Gamma \bar{Y}\, \varepsilon^*_\Gamma(x,y) = \frac{2}{3}\sqrt{3}\bar{Y}\, \Delta\Gamma_y \quad \ldots\ldots\ldots\ldots \quad (2.3)$$

Here $\bar{Y} = \bar{Y}(x,y)$ is the average Y, when in (x,y) on Γ the effective strain varies up to $\varepsilon^*(x,y)$; $\bar{\bar{Y}}$ is the average Y along Γ. Approximating $\varepsilon^*_\Gamma$ by $\frac{2}{3}\sqrt{3}\varepsilon_1$, along Γ, pending a refined plasticity analysis not pursued here, the last equation of (2.3) was written, with $\Delta\Gamma_y$ the elongation of the y-component of the original length $\Gamma_o$ of the Γ-curve. Comparing (2.3) with the well-known expression $R = \beta Y \delta$ , (with δ = crack opening displacement) a contribution to the interpretation of the in literature controversially discussed β appears to have been made. Approaching $Y = Y(\varepsilon^*)$ by $Y = k\varepsilon^{*n}$:

$$R = \int_\Gamma dy \frac{k\varepsilon^{*\,n+1}_\Gamma}{n+1} = \int_\Gamma \frac{k\varepsilon^{*\,n+1}_\Gamma(s)}{(n+1)\frac{d\varepsilon^*_\Gamma}{dy}} d\varepsilon^*_\Gamma = \frac{k\varepsilon^{*\,n+2}_{\Gamma,tip}}{(n+1)(n+2)\frac{d\varepsilon^*_\Gamma}{dy}} \quad \ldots\ldots \quad (2.4)$$

with $\frac{d\varepsilon^*_\Gamma}{dy}$ = effective strain gradient along Γ.

$$R = \frac{\varepsilon^*_{\Gamma,tip}}{n+2} e_{tip} \Big/ \overline{\frac{d\varepsilon^*_\Gamma}{dy}}, \quad \text{with } e_{tip} = \int_0^{\varepsilon^*_{\Gamma,tip}} k\varepsilon^{*n}_\Gamma d\varepsilon^*_\Gamma \quad \ldots\ldots \quad (2.5)$$

This relates R with $e_{tip}$, the effective strain at the tip, the effective strain hardening exponent and the (average) effective strain gradient in the plastic zone. The locus $\Gamma = \Gamma(x,y)$ can be approximated by straight lines from the crack tip to the points $P_{1,2}$ on the elastic plastic boundary $y_B = y_B(x)$ for which $\frac{dy_B}{dx} = 0$.

For sufficiently small plastic zone size $y_B(x)$ can be approximated from the goniometric (Sneddon) approximation of Westergaard's description of the stress configuration at the cracktip and the Von Mises flow criterion. One deduces for the polar equation $g_B(\theta)$ of the elastic plastic boundary:

$$\gamma(\theta) = \frac{g_B(\theta)}{a} = \Omega\cos^2\frac{\theta}{2}\left(1+3\sin^2\frac{\theta}{2}\right) \quad \ldots\ldots\ldots\ldots\ldots \quad (2.6)$$

with $\Omega = \frac{\sigma^2}{2Y^2}\left(1+\frac{\sigma^2}{2Y^2}\right)$ for $\sigma$ = gross stress, Y = uniaxial yield stress (and using the Irwin-correction $\frac{K^2}{2\pi Y^2}$ for half the plastic zone size to indicate the mathematical aequivalent crack).

In $P_{1,2}$ is $\frac{dy_B}{dx} = 0$ or $\frac{d\gamma}{d\theta} = -\gamma\frac{\cos\theta}{\sin\theta}$ $\ldots\ldots\ldots\ldots$ (2.7)

As also from (2.6): $\frac{d\gamma}{d\theta} = \frac{1}{2}\Omega\sin\theta(3\cos\theta - 1)$ $\ldots\ldots\ldots$ (2.8)

one has in $P_{1,2}$: $\gamma = \frac{1}{2}\Omega\frac{\sin^2\theta}{\cos\theta}(1-3\cos\theta)$ $\ldots\ldots\ldots$ (2.9)

From (2.6) and (2.9): $9\cos^3\theta - 4\cos^2\theta + 11\cos\theta + 2 = 0$ $\ldots$ (2.10)

For the intersections $P_{1,2}$ of $\Gamma$ with the elastic plastic boundary one thus finds:

$\theta = 79{,}9^0$ ; $\frac{\gamma}{\Omega} = 1.31$ ; $\frac{x}{\Omega} = 0.23$ ; $\frac{y}{\Omega} = 1.29$.

This implies that $\Gamma$ can be approximated by a line from a point of the plastic wake boundary towards the crack path under an angle of ca. $80^0$ with the crack direction. Of course shear lips and other irregularities will unfavourably interfere with the $R_a$-estimate according to (2.3) for which a mesh can be applied to the plate before fracture. For the dynamic situation the relevant $\gamma = \gamma(\dot{\varepsilon})$ diagram has to be used and the description of the elastic plastic boundary accordingly adapted.

## 3. THE EVALUATION OF THE CRACK EXTENSION RESISTANCE R FOR THE DUCTILE CASE UNDER DISPLACEMENT CONTROLLED CONDITIONS FROM ENERGY BALANCE CONSIDERATIONS

If a crack with length a extends in a plate (e.g. a CT specimen) submitted to a displacement rate $\dot{f}$ transversal to the crack, the energy balance offers:

$$\Delta A = P\Delta f = \left(\frac{\partial W}{\partial a}\right)_P \Delta a + \left(\frac{\partial W}{\partial P}\right)_a \Delta P + \left(\frac{\partial U}{\partial a}\right)_P \Delta a + \left(\frac{\partial U}{\partial P}\right)_a \Delta P + \left(\frac{\partial V}{\partial a}\right)_P \Delta a + \left(\frac{\partial V}{\partial P}\right)_a \Delta P \quad (3.1)$$

A = performed work
P = load
f = deflection
a = cracklength
U = elastic potential energy
V = kinetic energy
$W_e$ = energy dissipated during crack extension



The dissipated energy during crack extension $W_e$ can be separated in

$W_e = W_{ea} + W_{eq}$, with

$W_{ea}$ = dissipated energy required for crack extension

$W_{eq}$ = dissipated energy unavoidably accompanying $W_{ea}$ in a given dimensional and geometrical situation, if ductility is sufficiently present and due to the material reaction forces causing yield at the load values required for crack extension. ≠

$R = \frac{dW_e}{da}$ = 'apparent' fracture propagation resistance = $R_a + R_q$

$R_a = \frac{dW_{ea}}{da}$ = 'real' fracture propagation resistance

$R_q = \frac{dW_{eq}}{da}$ = 'reactive' fracture resistance

Be $f = f_U + f_W$ with $f_U$ = elastic reversible part of f
$f_W$ = plastic reversible part of f

From the recording of the (P,f,a)-relation in time (e.g. by filming of a, simultaneously with a usual electronic recording of P and f in time, cf. fig. 3.1, one has:

$$\Delta A = P\Delta f = P^2\frac{dC_U}{da}\Delta a + P^2\left\{\left(\frac{\partial C_W}{\partial a}\right)_P \Delta a + \left(\frac{\partial C_W}{\partial P}\right)_a \Delta P\right\} + PC_U\Delta P + PC_W\Delta P \quad \ldots\ldots (3.2)$$

Here $f = CP = f_U + f_W = C_U P + C_W P$, with
$C$ = compliance = $C_U + C_W$
$C_U = C_U(a)$ = elastic compliance
$C_W = C_W(a,P)$ = plastic compliance

Thus with $U = \frac{1}{2}C_U P^2$ from (3.1) and (3.2):

$$R_a = \left\{PC_W + P^2\left(\frac{\partial C_W}{\partial P}\right)_a\right\}\frac{dP}{da} + \frac{1}{2}P^2\frac{dC_U}{da} + P^2\left(\frac{\partial C_W}{\partial a}\right)_P - Q$$

$$Q \equiv \underbrace{\left\{\left(\frac{\partial W_{eq}}{\partial a}\right)_P + \left(\frac{\partial W_{eq}}{\partial P}\right)_a\frac{dP}{da}\right\}}_{R_q} + \underbrace{\left\{\left(\frac{\partial V}{\partial a}\right)_P + \left(\frac{\partial V}{\partial P}\right)_a\frac{dP}{da}\right\}}_{R_V} \quad \ldots\ldots\ldots\ldots (3.3)$$

Note: 1. For the elastic case and in absence of kinetic energy:

$$V = 0;\ C_W = 0;\ W_{eq} = 0;\ R = \frac{1}{2}P^2\frac{dC_U}{da} \equiv R_{aU} \quad \ldots\ldots\ldots\ldots (3.4)$$

the well-known l.e.f.m. result.

2. For the elastic-plastic case in absence of kinetic energy (e.g. performing experiments with a hydraulic slow loading equipment),

≠ If the reaction force over a ligament w-$a_o$ (or part $\alpha$(w-$a_o$) of it) is larger than Yb(w-$a_o$) (or $\alpha$b(w-$a_o$) resp.) the reaction force will cause yield.

and in absence of $W_{eq}$ (e.g. by suppression of $W_{eq}$, if otherwise being manifest, through stiffeners etc.) i.e. $V = 0$; $W_{eq} = 0$:

$$R = R_a = \underbrace{\tfrac{1}{2}P^2 \frac{dC_U}{da}}_{\longrightarrow} + \underbrace{P^2\left(\frac{\partial C_W}{\partial a}\right)_P + PC_W + P^2\left(\frac{\partial C_W}{\partial P}\right)_a \frac{dP}{da}}_{\longleftarrow}$$

$$= R_{aU} + R_{aW} \quad \ldots\ldots\ldots \quad (3.5)$$

(If $\left(\frac{\partial C_W}{\partial a}\right)_P / C_W + P\left(\frac{\partial C_W}{\partial P}\right)_a = -\frac{1}{P}\frac{dP}{da}$ or $f_W = C_W \cdot f$ = constant, in a certain region, then $R_{aW} = 0$ and $R = R_{aU}$, suggesting possibilities for assessment of l.e.f.m. values outside their field of validness conditions).

$C_U = C_U(a)$ can be found experimentally from a calibration specimen by recording of the (P,f,a)-relation at unloading and reloading for several crack extensions. The small hysteresis observed at these loading cycles is readily attributed to an energy dissipation by plastic compression in a region near the cracktip when unloading. This did not interfere with a sufficient estimate of $C_U$ from the slope of these cycles in the (P,f)-diagram. $C_U$ can also be numerically evaluated, using the finite elements method (for the elastic case). The agreement with the phenomenological method was usually excellent and the experimental calibration could (often) be discarded. Cf. fig. 3.2, 3.3.

In absence of kinetic energy terms $R = R_a + R_q$ as a function of a can be directly found from (3.3). For $C_U = C_U(a)$ can be assumed known, and thus $\frac{dC_U}{da}$, while from the (P,f)-diagram $C = C(f) = C(a)$ offers $C_W = C_W(a,P)$.
Cf. fig. 3.4a, 3.4b; 3.5 and fig. 3.6a, 3.6b.
Another even more direct evaluation, sometimes more suitable to fit the experimental data by the required curves, can proceed by:

$$W_e(a,a_o,w,h) = \int_{f_i}^{f_a} P\,df - \tfrac{1}{2}C_U(a)P^2 \quad \ldots\ldots\ldots\ldots\ldots\ldots (3.6a)$$

$$\text{and } R(a,a_o,w,h) = \frac{dW_e(a,a_o,w,h)}{da} \quad \ldots\ldots\ldots\ldots\ldots\ldots (3.6b)$$

($f_i$ = deflection at initiation, $\Delta a = 0$
$f_a$ = deflection at cracklength a ; $\Delta a = a - a_o$) Cf. fig. 3.7.

In presence of a substantial $R_q$, the evaluation of $R = R_a + R_q$, the apparent fracture resistance, as a function of a, or a/w, during tearing till total separation, shows that R usually rapidly decreases with increasing a in the initial phase, while in the terminal phase when the ligament approaches zero ($a/w \longrightarrow 1$), R will again clearly decrease (material to dissipate plastic energy ahead of the cracktip becomes less available). The disturbing influences of the initial and terminal phase of the crack extension (can) overlap in the



investigated a/w-interval and the R/a-curve might even not reveal an anticipated $R = R_a$-plateau, which presumably characterizes the 'real' fracture propagation resistance of the material. This R-plateau is then shrunk into an inflexion point, (with $\frac{d^2R}{da^2} = 0$, $\frac{d^3R}{da_3} < 0$ and $\frac{dR}{da} \leqslant 0$).
Examples of fractured specimens without stiffeners, with stiffeners and with stiffeners hinged outside the specimen opposite to the crack tip are shown in fig. 3.8 a,b,c,d.
When the initial notch was provided with a fatigued apex only a small decreasing effect on the R-values during the first phase of crack extension was observed. After a preambulary phase the R/a dependence appears rather independent of the initial notch size $a_o$. Side grooving introduced a clear lowering of the R/a-curve, as could be expected, while the suggestion of a plateau value was enhanced. Similar, though less pronounced effects, were introduced by the use of stiffeners intended to reduce 'q-dissipation', but apparently also interfering with 'a-dissipation'.

## 4. THE RELATION BETWEEN THE 'APPARENT' CRACK EXTENSION RESISTANCE R AND CRACK EXTENSION $(a-a_o)$ FOR THE DUCTILE CASE UNDER DISPLACEMENT CONTROLLED CONDITIONS

From the experimentally found qualitative behaviour of R vs $(a-a_o)$, cf. fig.3.1, follows that, if R is approximated by a polynomium in $(a-a_o)$, this is at least of third degree, thus:

$$R(a,a_o,w,h) = \sum_{k=0}^{\geqslant 3} R_k(a-a_o)^k \quad \text{with } R_k = R_k(a_o,w,h)$$

$$= R_0 + R_1(a-a_o) + R_2(a-a_o)^2 + R_3(a-a_o)^3 + \ldots \quad \ldots\ldots \quad (4.1)$$

while:

$$\frac{dR}{da} = \sum_{k=0}^{\geqslant 3} kR_k(a-a_o)^{k-1} < 0. \text{ An inflexion point occurs for:}$$

$$\frac{d^2R}{da^2} = \sum_{k=0}^{\geqslant 3} k(k-1)R_k(a-a_o)^{k-2} \simeq 2R_2 + 6R_3(a-a_o) = 0,$$

thus in $a^*$ with : $a^* - a_o \simeq -\frac{R_2}{3R_3} \quad \ldots\ldots\ldots\ldots\ldots\ldots\ldots\ldots (4.2a)$

while $R(a^*,a_o,w,h) = R^*(a_o,w,h) \simeq R_0 - \frac{R_2}{3R_3}\left(R_1 - \frac{2R_2^2}{9R_3}\right) \quad \ldots\ldots\ldots (4.2b)$

Corresponding with (3.1) the energy dissipated at crack extension, $W_e(a,a_o,w,h)$, if approximated by a polynomium in $(a-a_o)$, is at least of fourth degree:

$$W_e(a,a_0,w,h) = \sum_{k=0}^{\geq 3} \frac{R_k}{k+1} (a-a_0)^{k+1}$$

$$= R_0(a-a_0) + \frac{R_1}{2}(a-a_0)^2 + \frac{R_2}{3}(a-a_0)^3 + \frac{R_3}{4}(a-a_0)^4 + .. \quad (4.3)$$

Assuming:

$$R_k(a_0,w,h) = \sum_{j=0}^{\geq 3} R_{kj}(w-a_0)^j \text{ with } R_{kj} = R_{kj}(h)$$

$$= R_{k0} + R_{k1}(w-a_o) + R_{k2}(w-a_o)^2 + R_{k3}(w-a_0)^3 + \ldots \ldots \quad (4.4)$$

One will have:

$$R(a,a_0,w,h) = \sum_{k=0}^{\geq 3} \sum_{j=0}^{\geq 3} R_{kj}(a-a_0)^k(w-a_0)^j$$

$$= R_{00} + R_{01}(w-a_0) + R_{02}(w-a_0)^2 + R_{03}(w-a_0)^3 + \ldots$$

$$+ R_{10}(a-a_0) + R_{11}(w-a_0)(a-a_0) + R_{12}(w-a_0)^2(a-a_0) + \ldots$$

$$+ R_{20}(a-a_0)^2 + R_{21}(w-a_0)(a-a_0)^2 + \ldots$$

$$+ R_{30}(a-a_0)^3 + \ldots$$

$$\ldots\ldots\ldots \quad (4.5)$$

and:

$$W_e(a,a_0,w,h) = \sum_{k=0}^{\geq 3} \sum_{j=0}^{\geq 3} \frac{R_{kj}}{k+1} (w-a_0)^j(a-a_0)^{k+1}$$

$$= R_{00}(a-a_0) + R_{01}(w-a_0)(a-a_0) + R_{02}(w-a_0)^2(a-a_0) + R_{03}(w-a_0)^3(a-a_0) + \ldots$$

$$+ \frac{R_{10}}{2}(a-a_0)^2 + \frac{R_{11}}{2}(w-a_0)(a-a_0)^2 + \frac{R_{12}}{2}(w-a_0)^2(a-a_0)^2 + \ldots$$

$$+ \frac{R_{20}}{3}(a-a_0)^3 + \frac{R_{21}}{3}(w-a_0)(a-a_0)^3 + \ldots$$

$$+ \frac{R_{30}}{4}(a-a_0)^4 + \ldots$$

$$\ldots\ldots\ldots \quad (4.6)$$

(4.6) experimentally proves convex upwards in $(a-a_0)$, as further detailed in (4.2).

At complete separation:

$$W_e(a=w, a_0,w,h) = W_e(a_0,w,h) = \sum_{k=0}^{\geq 3} \rho_{e,k+1}(w-a_0)^{k+1}, \text{ with}$$

$$\rho_{e,k+1} = \sum_{j=0}^{k} \frac{R_{k-j,j}}{k+1-j} = R_{0,k} + \frac{R_{1,k-1}}{2} + \frac{R_{2,k-2}}{2} + \ldots + \frac{R_{k,0}}{k+1}$$

$$W_e(a_0,w,h) = R_{00}(w-a_0) + (R_{01} + \frac{R_{10}}{2})(w-a_0)^2 + (R_{02} + \frac{R_{11}}{2} + \frac{R_{20}}{3})(w-a_0)^3 +$$

$$+ (R_{03} + \frac{R_{12}}{2} + \frac{R_{21}}{3} + \frac{R_{30}}{4})(w-a_0)^4 + \ldots\ldots\ldots \quad (4.7)$$



(4.7) experimentally proves convex downwards in $(w-a_0)$, thus:

$$\sum_{k=0}^{\geq 3} (k+1)\rho_{e,k+1}(w-a_0)^k > 0 \; ; \; \sum_{K=0}^{\geq 3} k(k+1)\rho_{e,k+1}(w-a_0)^{k-1} > 0 \text{ or:}$$

$$R_{00} + 2R_{01} + R_{10}(w-a_0) > 0 \text{ and } 2R_{01} + R_{10} .. > 0 \ldots\ldots\ldots\ldots \quad (4.8)$$

It also proves from the experimental data, that $W_e(a_0,h,w)$ can be satisfactorily fitted, according to:

$$W_e(a_0,w,h) = \rho_1(w-a_0) + \rho_2(w-a_0)^2 \ldots\ldots\ldots\ldots\ldots\ldots \quad (4.9)$$

implying:

$$\rho_1 = R_{00} \; ; \; \rho_2 = R_{01} + \frac{R_{10}}{2} > 0 \text{ and } R_{kj} = 0 \text{ for } k+j > 2 \ldots\ldots \quad (4.10)$$

The total energy, including the initiation energy, to achieve the crack extension $(a-a_0)$ will be:

$$W(a,a_0,w,h) = W_i(a_0,w,h) + W_e(a,a_0,w,h) \ldots\ldots\ldots\ldots\ldots \quad (4.11)$$

Assume in analogy with (4.3):

$$W_i(a_0,w,h) = \sum_{k=0}^{\geq 3} \frac{r_k}{k+1}(w-a_0)^{k+1} \text{ with } r_k = r_k(h)$$

$$= r_0(w-a_0) + \frac{r_1}{2}(w-a_0)^2 + \frac{r_2}{3}(w-a_0)^3 + \frac{r_3}{4}(w-a_0)^4 + \ldots \quad (4.12)$$

then:

$$W(a,a_0,w,h) = \sum_{k=0}^{\geq 3} \{\frac{r_k}{k+1}(w-a_0)^{k+1} + \sum_{j=0}^{\geq 3} \frac{R_{kj}}{k+1}(w-a_0)^j(a-a_0)^{k+1}\}$$

$$= + \frac{R_{10}}{2}(a-a_0)^2 + \frac{R_{20}}{3}(a-a_0)^3 + \frac{R_{30}}{4}(a-a_0)^4 +$$

$$+(w-a_0)\{r_0 + R_{00} + R_{01}(a-a_0) + \frac{R_{11}}{2}(a-a_0)^2 + \frac{R_{21}}{3}(a-a_0)^3 + \frac{R_{31}}{4}(a-a_0)^4\} +$$

$$+(w-a_0)^2\{\frac{r_1}{2} + R_{02}(a-a_0) + \frac{R_{12}}{2}(a-a_0)^2 + \frac{R_{22}}{3}(a-a_0)^3 + \frac{R_{32}}{4}(a-a_0)^4\} +$$

$$+(w-a_0)^3\{\frac{r_2}{3} + R_{03}(a-a_0) + \frac{R_{13}}{2}(a-a_0)^2 + \frac{R_{23}}{3}(a-a_0)^3 + \frac{R_{33}}{4}(a-a_0)^4\} +$$

$$+(w-a_0)^4\{\frac{r_3}{4} + R_{04}(a-a_0) + \frac{R_{14}}{2}(a-a_0)^2 + \frac{R_{24}}{3}(a-a_0)^3 + \frac{R_{34}}{4}(a-a_0)^4\} +$$

$$\ldots\ldots \quad (4.13)$$

At complete separation:

$$W(a=w,a_0,w,h) = W(a_0,w,h) = \sum_{k=0}^{>3} \{\frac{r_k}{k+1} + \rho_{e,k+1}\}(w-a_0)^{k+1}$$

$$= (r_0 + R_{00})(w-a_0) + (\frac{r_1}{2} + R_{01} + \frac{R_{10}}{2})(w-a_0)^2 + (\frac{r_2}{3} + R_{02} + \frac{R_{11}}{2} + \frac{R_{20}}{3})(w-a_0)^3 + (\frac{r_3}{4} + R_{03} + \frac{R_{12}}{2} + \frac{R_{21}}{3} + \frac{R_{30}}{4})(w-a_0)^4 + \ldots$$

$$\ldots \quad (4.14)$$

It further proves from the experimental data, that: (Cf. fig. 4.1a and 4.1b): $W(a_0,w,h)$ can be satisfactorily fitted, according to:

$$W(a_0,w,h) = \rho_1^*(w-a_0) + \rho_2^*(w-a_0)^2 \quad \ldots \quad (4.15)$$

implying:

$$\rho_1^* = r_0 + R_{00} \; ; \; \rho_2^* = \frac{r_1}{2} + R_{01} + \frac{R_{10}}{2} \text{ and } R_{kj} = 0 \text{ for } k+j > 2 \quad \ldots \quad (4.16)$$

$W_i$ presumably contains a part $W_{iq}$ due to dissipative material reaction forces apart from the energy dissipation $W_{ia}$ at the cracktip required for crack initiation according to conventional fracture mechanics. As:

$$-\frac{dW_{ia}}{da_0} = \frac{dW_{ia}}{d(w-a_0)} = + r_{0a}$$ is the analogon of $J_{Ic}\{-\frac{dU_i}{da_0}\}$, $W_{iq}$ will be accounted for by $r_{q0}(w-a_0)$ and the other terms in $(w-a_0)^k$ with $\kappa > 1$, while $r_{ak} = 0$ for $k > 0$.

$$-\frac{dW_i}{da_0} = + r_{a0} + r_{q0} + r_{(q)1}(w-a_0) + r_{(q)2}(w-a_0)^2 \quad \ldots \quad (4.17)$$

is the 'apparent' $J_{Ic}\{-\frac{dU_i}{da_0}\}$ analogon. Separating $W_e$, and R as well, in their a- and q-contributions, (4.14) will read, if $R_{a,kj} = 0$ for $k+j > 1$.

$$\rho_1^* = J_{Ic} + r_{q0} + R_{a,00} + R_{q,00} \approx J_{Ic} + R_{a,00} \quad \ldots \quad (4.18)$$

$$2\rho_2^* = r_{q,1} + 2R_{q,01} + R_{q,10} \quad \ldots \quad (4.19)$$

For presumably $r_{q0}$ and $R_{q00}$ are zero, as this refers to energy density and not to an effective surface energy. In fact one can define the difference between a- and q-dissipation according to this.

If $J_{Ic}$ is determined according to the single test piece method, using the expression:

$$\frac{2H}{b(w-a_0)} = 2\frac{W_{ia} + W_{iq} + U}{b(w-a_0)} \quad \ldots \quad (4.20)$$

the discrepancy with the 'real' $J_{Ic}$ is $\frac{2W_{iq}}{b(w-a_0)}$



If $J_{Ic}$ is determined according to the multiple test piece method, using as an estimate:

$$-\frac{dH}{da_{0k}} = \frac{d(W_{ia} + W_{iq} + U_i)}{da_{0k}} \quad \ldots \quad (4.21)$$

with H is the absorbed energy at initiation for some $a_{0k}$-values, the discrepancy with the "real" $J_{Ic}$ is $-\frac{dW_{iq}}{da_{0k}}$.

If $H(a_{0k})$ is found by the 'open break' method, i.e. by extrapolation towards $(\Delta a_{0k})_i = 0$ of $H\{a_{0k} + (\Delta a_{0k})_i\}$ values for some $(\Delta a_{0k})_i$ one would expect in $a_{0k}$:

$$\{\frac{dH}{d(\Delta a_{0k})_i}\}(\Delta a_{0k})_i = 0 = \frac{dH}{da_{0k}} \quad \ldots \quad (4.22)$$

The discrepancy of $\frac{2H}{b(w-a_0)}$ (single test piece method) with the "real" $J_{Ic}$-value might be smaller than that of $-\frac{dH}{da_{0k}}$ (multiple test piece indication) with the 'real' $J_{Ic}$-value. For the latter will involve:

$$\frac{dW_{iq}}{da_{0k}} = \{\frac{dW_{eq}}{d(\Delta a_{0k})_i}\}(\Delta a_{0k})_i = 0 \gg \frac{dW_{ia}}{da_{0k}} = \{\frac{dW_{ea}}{d(\Delta a_{0k})_i}\}(\Delta a_{0k})_i = 0$$

while for the former: $W_{iq} \approx W_{ia}$

Conclusion:

It might finally be stated that the $R_a$-estimate as $R^* = R^*(a_0,w,h)$ at the inflexion point of the R vs $(a-a_0)$ - curve is corroborated by the independent $R_a$-estimate from $\frac{2}{3}\sqrt{3\bar{Y}}\,\Delta\Gamma_y$, with $\Delta\Gamma_y$ the maximum of $\Delta\Gamma_y = \Delta\Gamma_y(x)$ (in CT-specimens), these estimates providing fairly equal. Cf. fig. 4.2a, 4.2b. q-dissipative processes presumably will also effect $\Delta\Gamma_y$. In CT-specimens compression will decrease $\Delta\Gamma_y$ and the maximum $\Delta\Gamma_y$ near the cracktip appears to offer an acceptable estimate (as confirmed with $R^*$). In central notched specimen an overestimate of $\Delta\Gamma_y$ might result from the superposed plastic flow due to the material reaction forces (occurring if $Y(w-a_0)b < P$).

A previous communication on this subject was given in [8], to which is referred for preliminary experimental details; a more complete reporting also from the experimental side, is planned to follow next. Work related to the ideas sub 3 and sub 4 were communicated in [9], [10], [11] .

ACKNOWLEDGEMENTS

The above ideas were developed during activities for the phase IV part (laboratory test programme) of the European Pipeline Research Group (EPRG) programme on ductile fracture in gaspressurized pipelines. This was sponsored by the European Community for Steel and Carbon under convention 6210-46/6/601 and the EPRG-members Nederlandse Gasunie, British Gas Corporation and British Steel Corporation. We are indebted for fruitful discussions on the results by these sponsors. The investigations were carried through as a joint effort of Metal Research Institute TNO and British Steel Corporation, Product Technology, (of which Messrs Priest A and Holmes B, put forward e.g. eq 3.11).

REFERENCES

[1] Poynton, W.A. and Fearnehough, G.D., 'An analysis of shear fracture propagation in gas pipelines', Proc. of an International Conference on Dynamic Crack Propagation, Part III, p. 183, Lehigh University, Bethlehem, Pa., USA, July 1972.

[2] Proc. of the 1st International Conference on Crack Propagation in Pipelines, New Castle upon Tyne, England, 1974.
Cf. a.o.:
Paper 1 Poynton, W.A., 'A theoretical analysis of shear fracture propagation in backfilled gas pipelines'.
Paper 13 Mimura, H. and Ogasawara, M., 'Theoretical considerations on crack propagation in pipelines'.
Paper 14 Poynton, W.A., 'A theoretical analysis of shear fracture propagation in backfilled gas pipelines'.
Paper 15 Dick, J.A., Jamieson, P.McK. and Walker, E.F., 'The prediction of toughness requirements for the arrest of unstable fracture in pipelines'.
Paper 17 Shannon, R.W.E. and Wells, A.A., 'A study of ductile crack propagation in gas pressurized pipelines'.
and other papers.

[3] Hahn, G.T., Sarrate, M., Kanninen, M.F., and Rosenfield, A.R., Int. Journal of Fracture, Vol. 9, no. 2, 209, 1973.

[4] Maxey, W.A., Kiefner, J.F., Eiber, R.J. and Duffy, A.R., 'Ductile fracture initiation, propagation and arrest in cylindrical vessels, fracture toughness', Proc. of the 1971 Nat. Symposium on Fracture Mechanics, Part II, ASTM STP 514, 70, 1972.



[5] Kanninen, M.F. and Sampath, S.G., 'Crack propagation in pressurized pipelines', 2nd Int. Conference on Pressure Vessel Technology, San Antonio, Texas, USA, II-69, 1973, pp. 971-979.

[6] Kiefner, J.F., Maxey, W.A., Eiber, R.J., and Duffy, A.R., 'Failure stress levels of flaws in pressurized cylinders, progress in flaw growth and fracture toughness testing', Proc. of 6th Nat. Symposium on Fracture Mechanics, Philadelphia, 1972, ASTM STP 536, 1973, pp. 461-481.

[7] Elst, H.C. van, 'Criteria for steady state crack extension in gas pipelines', Proc. of Int. Conference on Prospects of Fracture Mechanics - Delft 1974, (Ed. G.C. Sih, H.C. van Elst, D. Broek - Noordhoff International Publishing - Leyden).

[8] Elst, H.C. van, Wildschut, H., Lont, M.A. and Toneman, F.H., 'The evaluation of the resistance against ductile crack extension', Proc. of Fracture 1977, ICF 4, Waterloo, Canada, Vol. 3 Part IV, pp. 155-167.

[9] Garwood, S.J., Robinson, J.N., and Turner, C.E., Int. Journal of Fracture 11, 1975, 528

[10] Mai, Y.W., Atkins, A.J., and Caddell, R.M., Int. Journal of Fracture 12, 1976, 391.

[11] Fearnehough, G.D., Dickson, D.T., and Jones, D.G., Int. Conference on Dynamic Fracture Toughness (paper 29), London, July 5 - 7, 1976.

CAPTIONS TO FIGURES

2.1 The development of the plastic wake of an extending crack by the sweeping of the locus of maximal energy density on lines parallel to the crack within the plastic zone.

3.1a Results of synchroneous load, deflection and cracklength recordings for CT-specimens (with and without stiffeners).

b Ditto, including crack velocity.

3.2 Experimental evaluation of elastic compliance as a function of cracklength (partial) unloading and reloading for some increasing crack extensions at recording of the load-deflection diagram.

3.3 Elements distribution used for numerical evaluation of dependence of elastic compliance on cracklength, using f.e.m. with a suitable substructuring technique.

3.4a Comparison of calculated elastic compliance as a function of crack-length using f.e.m. and experimental evaluation.

b Ditto, including side grooved specimens.

3.5 Elastic and plastic compliance as a function of cracklength.

3.6a Evaluation of energy dissipation per unit crack extension from eq (3.5).

b Ditto, averaged over some specimens for 3 materials.

3.7 Dissipated energy as a function of cracklength according to eq (3.6a).

3.8 Examples of tested specimens without and with stiffeners and with stiffeners, hinged outside the specimen (a,b,c,d resp.).

4.1a Dissipated energy for total separation as function ligament.

b Average energy dissipation per unit cracklength as a function of ligament and influence of strain rate (results mostly obtained by BSC-PT).

4.2a Elongation by plastic wake of propagated fracture transversal to crack direction as a function of distance to load line and for several gauge lengths after total separation for CT-specimen.

b Ditto, as a function of gauge length with distance to load line as parameter.

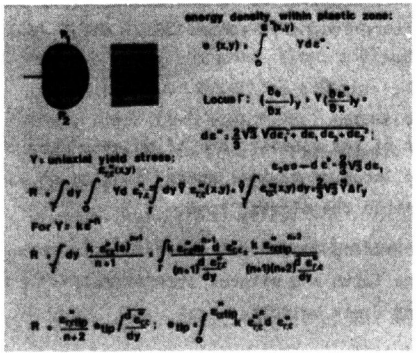


2.1



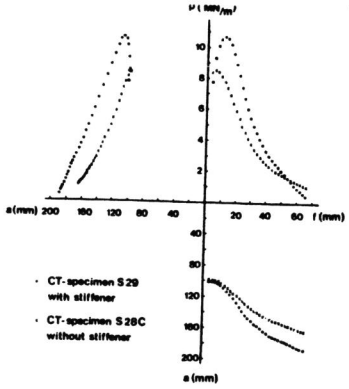


3.1a

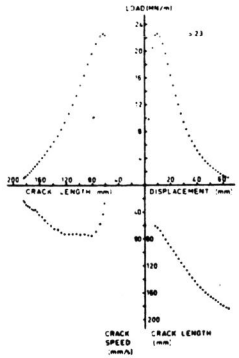


3.1b

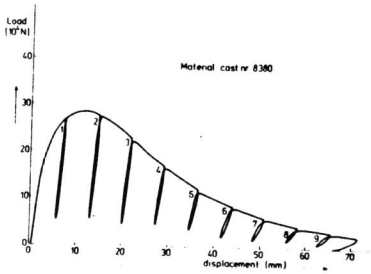


3.2

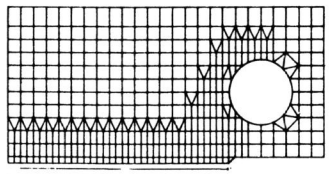

3.3

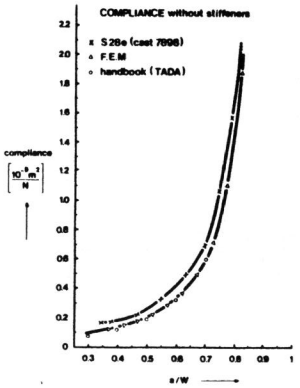


3.4a

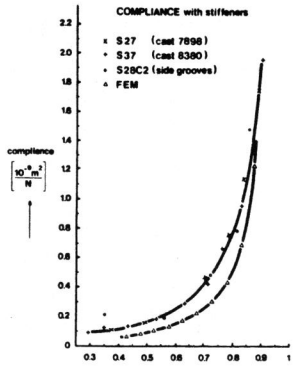


3.4b

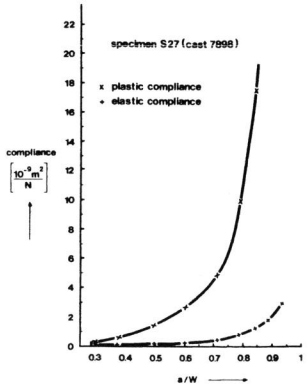


3.5

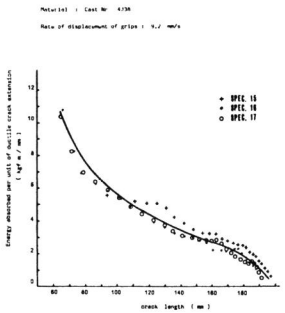


3.6a

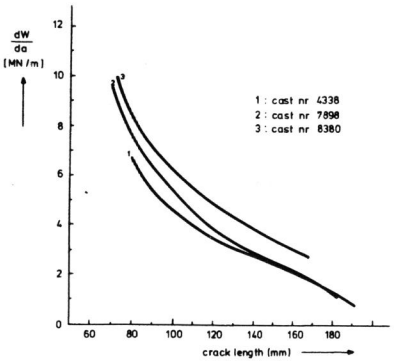


3.6b

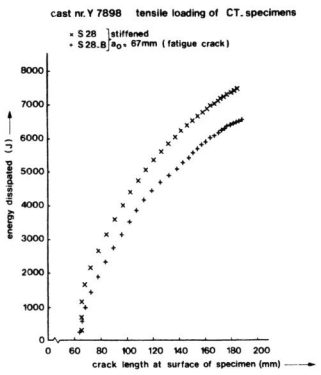


3.7

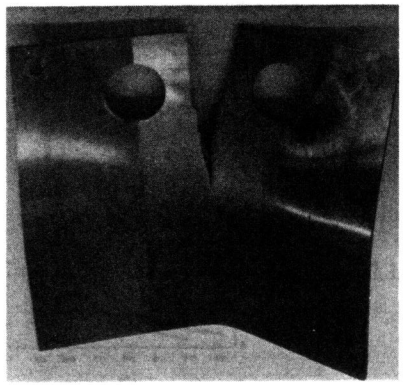

3.8a

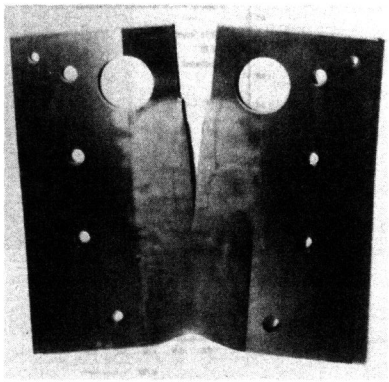

3.8b



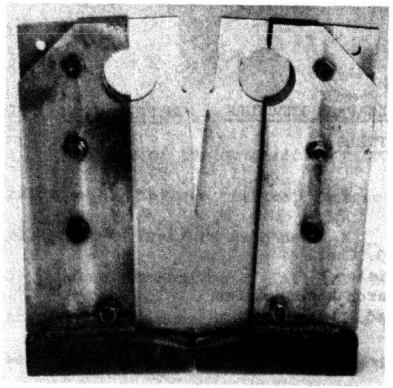

3.8c

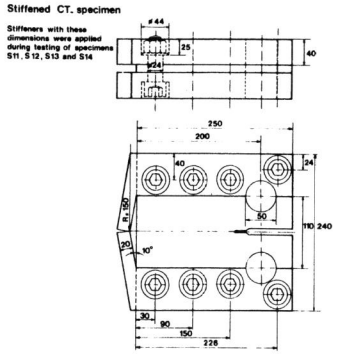


3.8d

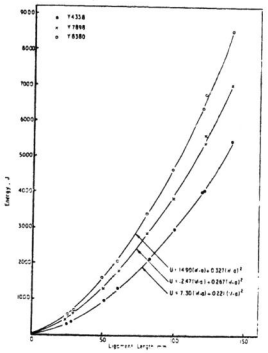


4.1a

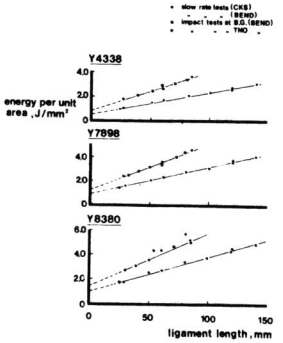


4.1b

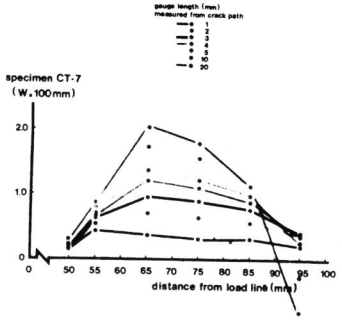


4.2a

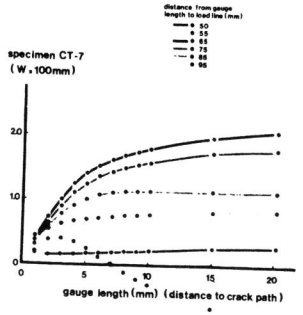


4.2b